

# Dielectric Rod Antenna for Glass-Packaged Radar Sensors at G-band

Thomas Galler<sup>#</sup>, Philipp Hügler<sup>\*</sup>, Tobias Chaloun<sup>#</sup>, Christian Waldschmidt<sup>#</sup>

<sup>#</sup>Institute of Microwave Engineering, Ulm University, Germany

<sup>\*</sup>Endress+Hauser SE+Co. KG, Germany

thomas.galler@uni-ulm.de

**Abstract**— A wideband and robust design of a dielectric rod antenna at G-band (140 GHz–220 GHz) for short range radar applications in harsh environmental conditions is presented. The proposed antenna is based on a simple plug-in solution made of PEEK material ( $\epsilon_{r,PEEK}=3.2$ ), which enables the mechanically detachable integration into a glass-encapsulated millimeter wave radar sensor system. To further increase the antenna gain, an optically transparent biconvex lens is presented. The antenna performance has been investigated by full wave simulations and validated through measurements of the fabricated antenna prototype. The experimental results of the realized antenna element show excellent agreement to the simulated values. The rod antenna covers a 3 dB-beam width of  $46^\circ$  and achieves a maximum gain of 12.4 dBi. The additional use of the dielectric lens increases the gain to 30.4 dBi with a stable beam pattern over the entire modulation bandwidth of 20 GHz of the radar sensor. The measured 3D-radiation patterns at various frequencies across the operational band are provided.

**Keywords**— rod antenna, glass, TGV, package, dielectric lens, MMIC, radar.

## I. INTRODUCTION

The trend of monolithic microwave integrated circuits (MMICs) towards higher frequencies due to the continuous development of silicon-germanium (SiGe) technology requires ever more highly integrated packaging concepts for miniaturized sensor systems [1]. Frequencies above 100 GHz provide large absolute bandwidths leading to a high range resolution. However, this places high demands on the assembly and integration technology [2], [3]. In solutions for radar sensors with on-chip antennas a considerable part of the system complexity is absorbed in chip development but at the expense of a low antenna efficiency and a complex and therefore expensive manufacturing process [4], [5].

This paper presents for the first time a complete primary radiator rod antenna uniformly illuminating a dielectric lens for a glass-packaged radar sensor. The rod is manufactured by a milling process but can also be fabricated by injection molding, which makes it a highly efficient and low-cost assembly. Unlike recently published designs [6], [7], [8], the presented design enables a continuous conversion between primary radiation and coupling into a dielectric waveguide [9], since it is only fixed by a plug-in connection without additional adhesive. Since the radiating element is intended to be used with a hermetically sealed radar sensor package for harsh environmental application like high temperature, humidity, or high pressure, a mechanical robust design is of importance.

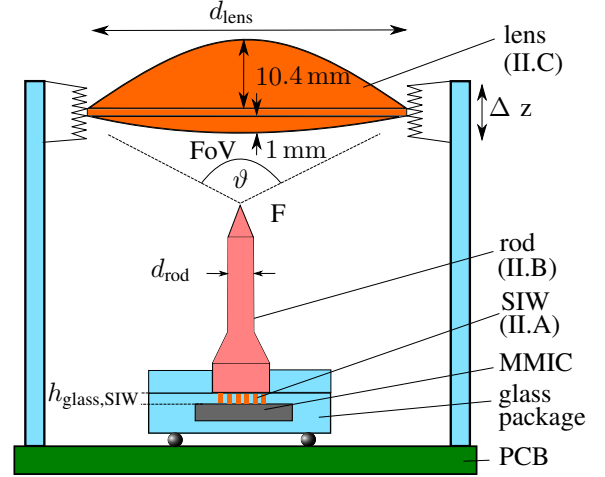


Fig. 1. Radar sensor in glass package and dielectric rod antenna illuminating a biconvex lens.

Additionally, the antenna gain can be further increased by the use of a dielectric lens fabricated in acrylic glass. Due to the resulting optical transparency, visual quality checks of the complete assembly can be made without further use of X-ray.

## II. ANTENNA PRINCIPLE

Based on the packaging concept for a hermetically sealed radar MMIC at 160 GHz presented in [9], a dielectric rod antenna illuminating a dielectric lens is developed for highly efficient radiation. The design is optimized for a low loss transition and high gain. The proposed antenna concept with the hermetically sealed MMIC is illustrated in Fig. 1. This allows a mechanically detachable and switchable connection from glass package to dielectric rod. Using a plug-in connection makes this a simple and low cost approach without the use of additional adhesive material. Using a biconvex lens fabricated in acrylic glass material performs a second stage of beam focusing enabling higher measurement ranges for radar applications.

### A. SIW transition and on-chip excitation

The RF output on the radar MMIC is a microstrip line with an U-shaped galvanically coupled structure as a transition from chip to glass layer ②, presented in [9]. This feeds a substrate integrated waveguide (SIW) structure realized in the 100  $\mu\text{m}$  thick layer of glass ( $h_{\text{glass,SIW}}$ ). The SIW is laterally bounded

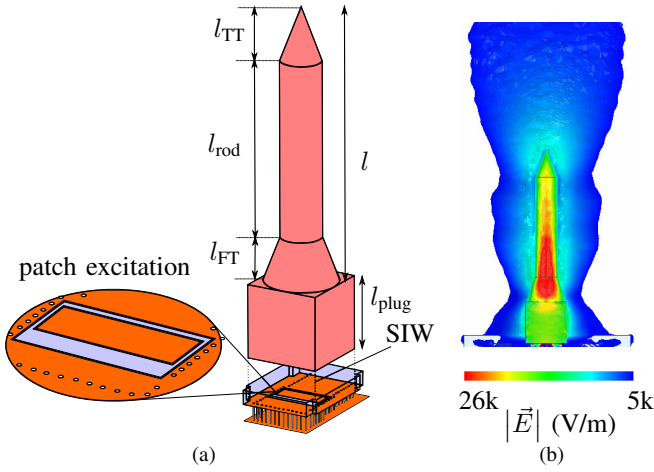


Fig. 2. Perspective view of the dielectric rod in the glass cavity; (a) excitation, (b) electric field distribution along the vertical cross section of the rod antenna.

by through-glass vias (TGVs) with a diameter of  $20\text{ }\mu\text{m}$  and a pitch of  $65\text{ }\mu\text{m}$ . As the distance between the vias is  $< \lambda_G/10$  they act as electric walls. The metalization on the glass consists of a  $10\text{ nm}$  seed layer of NiCr and a subsequent sputtered copper layer ( $4\text{ }\mu\text{m}$ ). A rectangular recess on the top metal layer of the SIW is inserted, including a patch antenna to feed the dielectric rod antenna. The dimensions of the radiating patch determine the center frequency and thus the excitation of the dielectric PEEK rod with the fundamental  $\text{HE}_{11}$  mode. The position of the PEEK rod is aligned over the patch antenna in such a way, the electromagnetic field coupling from the SIW to the rod is optimized for the excitation of the fundamental mode  $\text{HE}_{11}$ .

### B. PEEK rod antenna

Based on the SIW transition and the excitation structure, a circular dielectric PEEK rod is presented in Fig. 2 (a). By using a dielectric rod as a primary radiator, high gain is achieved on the effect of a smaller beam width. To decrease the insertion loss and apply an easy detachable connection in the glass package, an additional rectangular PEEK section with an edge length of  $(1\text{ mm} \times 1\text{ mm} \times 1\text{ mm})$  is added. Additionally, impedance matching is achieved by optimizing  $l_{\text{plug}}$ . Due to the mechanically decoupled connection, the rod can be exchanged directly with a flexible dielectric waveguide as shown in [9]. By means of full-wave simulation, the dimensions of the rod are determined. A conical feed with a diameter of  $1\text{ mm}$  tapered to  $d_{\text{rod}} = 550\text{ }\mu\text{m}$  and length  $l_{\text{FT}}$  is used to stimulate the surface wave along the rod. Fig. 2 (b) depicts the electric field distribution of the rod antenna. The guidance of the surface wave mode is determined by the radius of the rod and thus optimized for the operating frequency of  $168\text{ GHz}$ , as illustrated in Fig. 3. Assuming a desired gain of  $10\text{ dBi}$  to  $15\text{ dBi}$  a minimum side lobe level can be achieved with the approach described in [10]. An optimum is found at a length 3–7 times the wavelength. This design has a length of  $l_{\text{rod}} = 2.4\text{ mm}$ . Using this length, the ratio of  $\frac{\lambda_0}{\lambda_{\text{surface}}}$  determines the final radius of the rod. [10] uses the mean value of

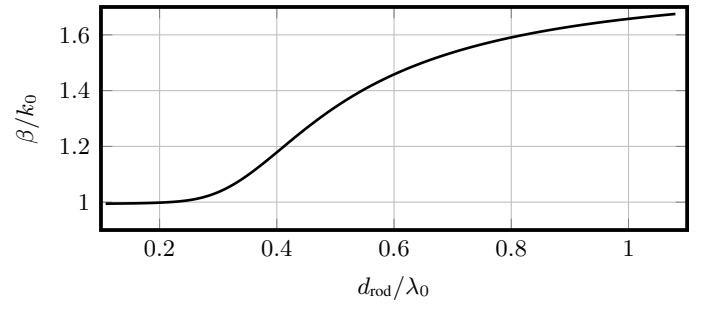


Fig. 3. Simulated normalized phase constant over the normalized rod diameter for the  $\text{HE}_{11}$  mode at  $168\text{ GHz}$ .

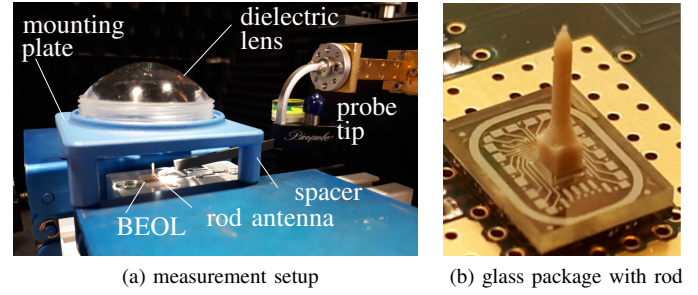


Fig. 4. Sensor setup with the rod clamped in the glass package.

maximum efficiency ( $p=6$ ) and an optimum in phase difference without feed taper ( $p=3.618$ )

$$\frac{\lambda_0}{\lambda_{\text{surface}}} = 1 + \frac{\lambda_0}{p \cdot l}. \quad (1)$$

The length of the terminal taper  $l_{\text{TT}} \approx \frac{\lambda_{\text{surface}}}{2}$  and the feed taper  $l_{\text{FT}} \approx \frac{1}{5}l$  are set to  $750\text{ }\mu\text{m}$  and  $600\text{ }\mu\text{m}$ , respectively. With a total length of  $3.7\text{ mm}$ , the rod forms a very compact antenna integrated in the glass sensor package. The rod was milled from one piece of PEEK material and clamped into the cavity of the glass package. The measurement setup using a back-end-of-line (BEOL) chip is illustrated in Fig. 4 (a). From the simulation the rod antenna provides a  $3\text{ dB}$ -beam width of  $50^\circ$  in E-plane and  $48^\circ$  in H-plane, as depicted in Fig. 5. In the next step, the far field measurements of the PEEK rod antenna was conducted using a robot-supported millimeter-wave test range [11], [12]. The measured radiation pattern is illustrated for elevation angles between  $-30^\circ$  and  $30^\circ$  in both planes. A  $3\text{ dB}$ -beam width of  $46^\circ$  in E-plane,  $40^\circ$  in H-plane, and a maximum gain of  $12.4\text{ dBi}$  were measured at the frequency of  $168\text{ GHz}$ . To reduce the influence on the radiation pattern of the antenna, a probe tip with an extended shaft is used. The measured 3D-radiation pattern in Fig. 6 shows a uniform beam pattern in all azimuth planes, which coincides very good with the simulation results. The measured reflection coefficient illustrated in Fig. 7 is below  $-10\text{ dB}$  across a wide frequency range of  $152\text{ GHz}$ – $174\text{ GHz}$ . Additionally, the influence of the probe tip is removed by means of time gating. With regard to the intended use of the PEEK rod antenna as the primary feed, uniform illumination of a dielectric lens is possible.

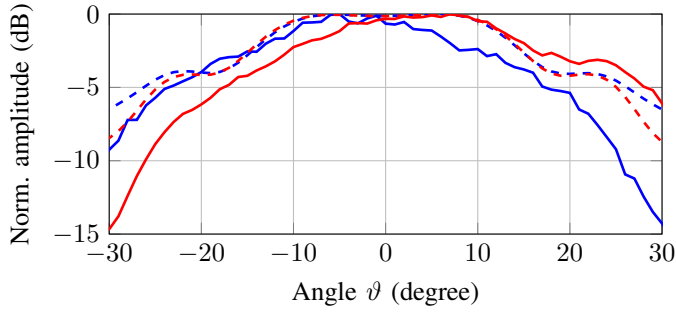


Fig. 5. Radiation pattern of the dielectric rod antenna. (—  $E_{\text{sim}}$ , —  $E_{\text{meas}}$ , —  $H_{\text{sim}}$ , —  $H_{\text{meas}}$ )

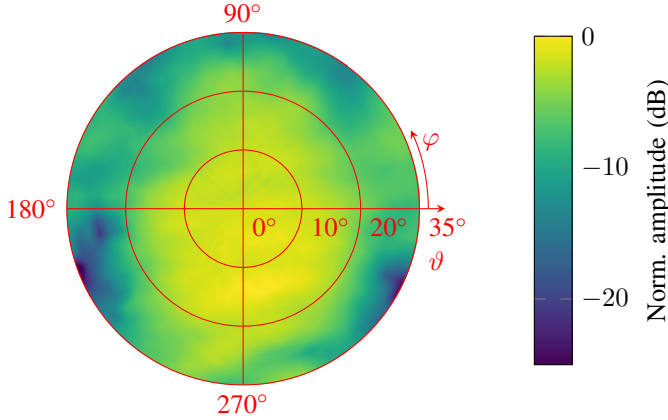


Fig. 6. Measured 3D-radiation pattern of the dielectric rod antenna without lens at 168 GHz.

### C. Beam focusing dielectric lens

A further increase of the gain is achieved by use of a biconvex lens illuminated by the dielectric rod antenna. To enable a visual transparency and view on the glass package, acrylic glass is used as a substrate material. The design is based on a quasi optical approach with the feeding point in the focal point F, as illustrated in Fig. 1. Acrylic glass has a permittivity of  $\epsilon_{r,\text{lens}}=2.26$  which determines the refractive index to

$$n = \sqrt{\epsilon_{r,\text{lens}}} = 1.5. \quad (2)$$

The diameter of the lens is set to 36 mm with a maximum thickness of 14.4 mm. For optical transparency, the lens is polished without any additional influence on the refractive behavior. For full illumination by the PEEK rod, the lens is designed for a distance of 28 mm. A biconvex design of the antenna is used to reduce the construction depth in terms of the distance to the focal point. The first convex lens with a thickness of 1 mm bundles the beam of the rod antenna. Secondly, an additional convex lens with a thickness of 10.4 mm bundles the beam to an angular range  $|\theta| < 2.5^\circ$ . All corresponding dimensions are listed in Tab. 1. A mounting plate is used to align the biconvex lens over the rod antenna with the spacer for vertical distance variation. Using the screw tread, the lens distance can be adjusted to the correct focal point F.

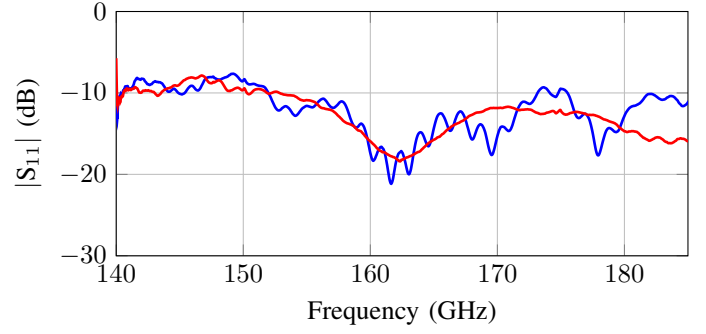


Fig. 7. Measured reflection coefficient of the realized glass antenna. (— original data, — data without probe tip)

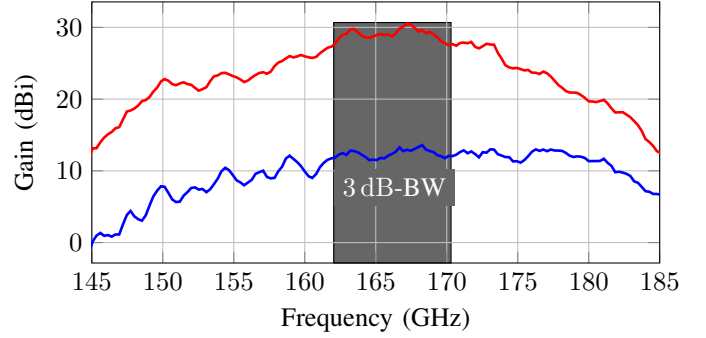


Fig. 8. Measured gain for the realized rod antenna in glass package. (— without lens, — with lens)

Table 1. Final dimensions for the dielectric rod in the glass package and the biconvex lens.

$l_{\text{TT}}$	750 $\mu\text{m}$	$l_{\text{rod}}$	2.4 mm	$l_{\text{FT}}$	600 $\mu\text{m}$
$l_{\text{plug}}$	1 mm	$d_{\text{rod}}$	550 $\mu\text{m}$	F	28 mm
$d_{\text{lens}}$	36 mm	$h_{\text{glass,SIW}}$	100 $\mu\text{m}$	$\vartheta$	46°
$\Delta z$	10 mm	—	—	—	—

Fig. 8 shows the measured gain of the antenna prototype as a function of frequency. The maximum antenna gain is measured to 12.4 dBi for the PEEK rod and 30.4 dBi at 168 GHz with the dielectric lens, respectively. The measured 3D-radiation patterns at different frequencies across the 3 dB-bandwidth of the transition in [9] are shown in Fig. 9. Since the SIW excitation of the proposed rod antenna has an operational bandwidth of 155 GHz–175 GHz a stable far field diagram is expected, which could also be confirmed by the measurements. Exemplary, the measured radiation pattern in the E- and H-plane at 168 GHz are shown in Fig. 10. Apart from a slight asymmetry observed in the H-plane of the measured radiation characteristics of the antenna prototype, a strong focus in the far field diagrams can be stated in both planes. These differences stem from parasitic radiations of the probe tip and unwanted interactions with the test environment. The obtained 3 dB-beam width is  $5^\circ$  in the E-plane and  $4^\circ$  in the H-plane with a sidelobe level of 13 dB, respectively. A comparison to other state-of-the-art rod antenna solutions is listed in Tab. 2.

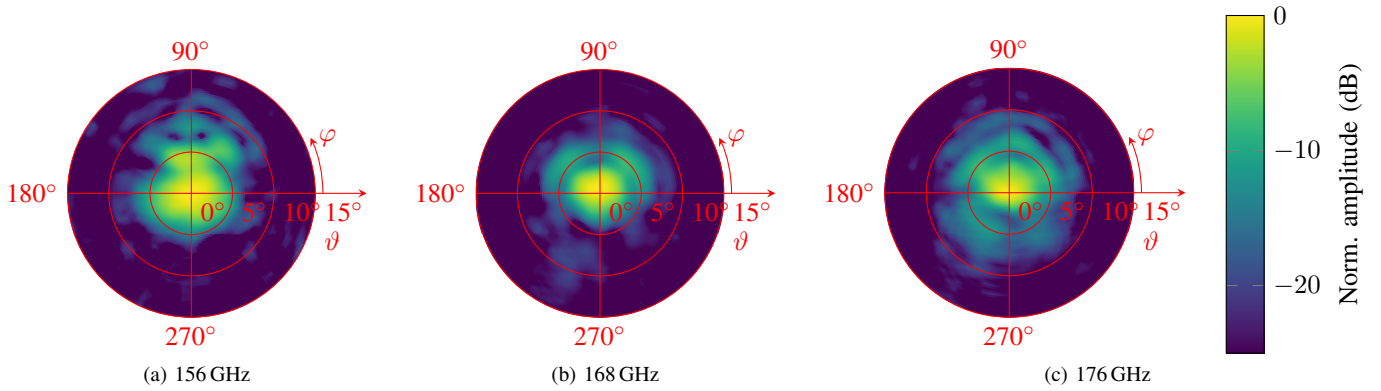


Fig. 9. Measured 3D-radiation patterns of the dielectric rod antenna with lens at different frequencies (E-/H-plane:  $\varphi = 0^\circ/90^\circ$ ).

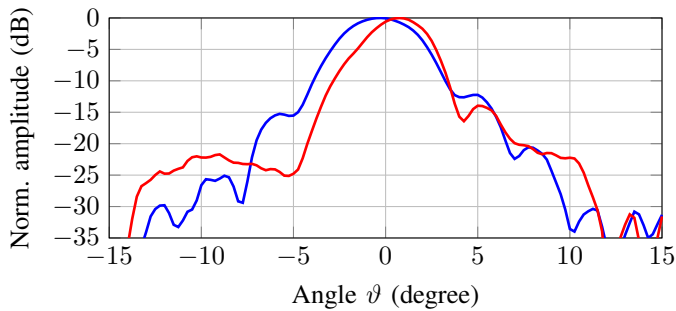


Fig. 10. Measured radiation pattern of dielectric rod and lens antenna. (— E-plane, — H-plane)

Table 2. Comparison to state-of-the-art rod antennas.

Literature	Gain (dBi)	$f$ (GHz)	3 dB-BW (deg)	$\epsilon_r$	length (mm)
this work	12.4	168	46	3.2	3.7
this work + lens	30.4	168	5	3.2	34
[6]	10.3	160	56	12.9	23
[7]	10	102	60	9.6	7

### III. CONCLUSION

A dielectric rod antenna at G-band is presented, suitable for short range distance measurement in harsh environmental scenarios. A key aspect of this antenna design is its simple mechanical detachable connection with a glass-packaged radar sensor. This has been verified through the realization and characterization of the rod antenna fabricated in PEEK material. The spherical radiation characteristics of the antenna up to elevation angles of  $\pm 35^\circ$  has been validated in the frequency band from 156 GHz to 176 GHz using a robot-supported millimeter wave test range. To further increase the gain, an optical transparent biconvex lens is used. The rod antenna prototype uniformly illuminating the lens shows excellent agreement between the measured and simulated radiation pattern. The measured radiation patterns show a maximum antenna gain of 12.4 dBi for the rod antenna and 30.4 dBi with the additional lens.

### ACKNOWLEDGMENT

This work was funded by the VDI/VDE Innovation + Technik GmbH within the project GlaRA. – 16ES0692

### REFERENCES

- [1] M. Hitzler, P. Grüner, L. Boehm, W. Mayer, and C. Waldschmidt, "On Monostatic and Bistatic System Concepts for mm-Wave Radar MMICs," *IEEE Transactions on Microwave Theory and Techniques*, vol. 66, no. 9, pp. 4204–4215, 2018.
- [2] T. Jaeschke, C. Bredendiek, and N. Pohl, "A 240 GHz ultra-wideband FMCW radar system with on-chip antennas for high resolution radar imaging," in *IEEE MTT-S International Microwave Symposium Digest (MTT)*, Jun. 2013, pp. 1–4.
- [3] A. Bhutani, B. Goettel, M. Pauli, and T. Zwick, "122 GHz FMCW Radar System-in-Package in LTCC Technology," in *2019 16th European Radar Conference (EuRAD)*, 2019, pp. 373–376.
- [4] M. Hitzler, P. Grüner, L. Boehm, W. Mayer, and C. Waldschmidt, "On Monostatic and Bistatic System Concepts for mm-Wave Radar MMICs," *IEEE Transactions on Microwave Theory and Techniques*, vol. 66, no. 9, pp. 4204–4215, Sep. 2018.
- [5] W. Khan and et al., "A D-Band Micromachined End-Fire Antenna in 130-nm SiGe BiCMOS Technology," *IEEE Transactions on Antennas and Propagation*, vol. 63, no. 6, pp. 2449–2459, 2015.
- [6] A. A. Generalov, J. A. Haimakainen, D. V. Lioubtchenko, and A. V. Räisänen, "Wide band mm- and sub-mm-wave dielectric rod waveguide antenna," *IEEE Transactions on Terahertz Science and Technology*, vol. 4, no. 5, pp. 568–574, 2014.
- [7] N. Ghassemi and K. Wu, "Planar Dielectric Rod Antenna for Gigabyte Chip-to-Chip Communication," *IEEE Transactions on Antennas and Propagation*, vol. 60, no. 10, pp. 4924–4928, 2012.
- [8] G. L. Saffold and T. M. Weller, "Dielectric rod antenna array with planar folded slot antenna excitation," *IEEE Open Journal of Antennas and Propagation*, vol. 2, pp. 664–673, 2021.
- [9] T. Galler, T. Chaloun, W. Mayer, K. Kröhnert, D. Starukhin, N. Ambrosius, M. Schulz-Ruhtenberg, and C. Waldschmidt, "Glass Package for Radar MMICs Above 150 GHz," *IEEE Journal of Microwaves*, pp. 1–11, 2021.
- [10] B. Heverlee, S. Y. Stroobandt, and I. S. Stroobandt, *An X-Band High-Gain Dielectric Rod Antenna*, Belgium, Ed., 1997.
- [11] L. Boehm, F. Boegelsack, M. Hitzler, and C. Waldschmidt, "The Challenges of Measuring Integrated Antennas at Millimeter-Wave Frequencies [measurements corner]," *IEEE Antennas and Propagation Magazine*, vol. 59, no. 4, pp. 84–92, Aug. 2017.
- [12] —, "Enhancements in mm-wave antenna measurements: automatic alignment and achievable accuracy," *IET Microwaves, Antennas & Propagation*, no. 11, pp. 1676–1680, 2017.